GLOBAL BIOGEOCHEMICAL CYCLES, VOL. 19, GB2019, doi:10.1029/2004GB002366, 2005

Fire emissions from C_3 and C_4 vegetation and their influence on interannual variability of atmospheric CO_2 and $\delta^{13}CO_2$

J. T. Randerson,[1] G. R. van der Werf,[2,3] G. J. Collatz,[4] L. Giglio,[5] C. J. Still,[6] P. Kasibhatla,[7] J. B. Miller,[8,9] J. W. C. White,[10] R. S. DeFries,[11,12] and E. S. Kasischke[11]

Received 1 September 2004; revised 7 January 2005; accepted 16 March 2005; published 7 May 2005.

[1] Measurements of atmospheric trace gases provide evidence that fire emissions increased during the 1997/1998 El Niño event and these emissions contributed substantially to global CO_2, CO, CH_4, and $\delta^{13}CO_2$ anomalies. Interpretation and effective use of these atmospheric observations to assess changes in the global carbon cycle requires an understanding of the amount of biomass consumed during fires, the molar ratios of emitted trace gases, and the carbon isotope ratio of emissions. Here we used satellite data of burned area, a map of C_4 canopy cover, and a global biogeochemical model to quantitatively estimate contributions of C_3 and C_4 vegetation to fire emissions during 1997–2001. We found that although C_4 grasses contributed to 31% of global mean emissions over this period, they accounted for only 24% of the interannual emissions anomalies. Much of the drought and increase in fire emissions during the 1997/1998 El Niño occurred in tropical regions dominated by C_3 vegetation. As a result, the $\delta^{13}CO_2$ of the global fire emissions anomaly was depleted (−23.9‰), and explained approximately 27% of the observed atmospheric decrease in $\delta^{13}CO_2$ between mid-1997 and the end of 1998 (and 61% of the observed variance in $\delta^{13}CO_2$ during 1997–2001). Using fire emissions that were optimized in an atmospheric CO inversion, fires explained approximately 57% of the observed atmospheric $\delta^{13}CO_2$ decrease between mid-1997 and the end of 1998 (and 72% of the variance in $\delta^{13}CO_2$ during 1997–2001). The severe drought in tropical forests during the 1997/1998 El Niño appeared to allow humans to ignite fires in forested areas that were normally too moist to burn. Adjacent C_4 grasses (in woodlands and moist savannas) also burned, but emissions were limited, in part, by aboveground biomass levels that were 2 orders of magnitude smaller than C_3 biomass levels. Reduced fuel availability in some C4 ecosystems may have led to a negative feedback on emissions.

Citation: Randerson, J. T., G. R. van der Werf, G. J. Collatz, L. Giglio, C. J. Still, P. Kasibhatla, J. B. Miller, J. W. C. White, R. S. DeFries, and E. S. Kasischke (2005), Fire emissions from C_3 and C_4 vegetation and their influence on interannual variability of atmospheric CO_2 and $\delta^{13}CO_2$, *Global Biogeochem. Cycles*, *19*, GB2019, doi:10.1029/2004GB002366.

1. Introduction

[2] For the most part, grasses and trees in tropical ecosystems have different photosynthetic pathways (C_4 and C_3) that lead to distinct differences in their carbon isotope ratios [*Sage and Monson*, 1999]. These relatively large isotopic differences allow for partitioning of respiration and photosynthesis fluxes between these two plant functional types in ecosystems that have a mixed C_3 and C_4 canopy [*Ometto et al.*, 2002; *Still et al.*, 2003b] and for the estimation of soil carbon residence times in ecosystems that have undergone a shift from one pathway type to the other [*Martin et al.*, 1990; *Veldkamp*, 1994; *Townsend et al.*,

[1]Department of Earth System Science, University of California, Irvine, California, USA.
[2]U.S. Department of Agriculture Foreign Agriculture Service (USDA-FAS), NASA Goddard Space Flight Center, Greenbelt, Maryland, USA.
[3]Now at Faculty of Earth and Life Sciences, Vrije Universiteit, Amsterdam, Netherlands.
[4]NASA Goddard Space Flight Center, Greenbelt, Maryland, USA.
[5]Science Systems and Applications Inc., Greenbelt, Maryland, USA.
[6]Geography Department, University of California, Santa Barbara, California, USA.
[7]Nicholas School of the Environment and Earth Sciences, Duke University, Durham, North Carolina, USA.
[8]NOAA Climate Monitoring Diagnostics Laboratory, Boulder, Colorado, USA.
[9]Also at Cooperative Institute for Research in Environmental Science, University of Colorado, Boulder, Colorado, USA.
[10]Cooperative Institute of Arctic and Alpine Research, University of Colorado, Boulder, Colorado, USA.
[11]Department of Geography, University of Maryland, College Park, Maryland, USA.
[12]Also at Earth System Science Interdisciplinary Center, University of Maryland, College Park, Maryland, USA.

0886-6236/05/2004GB002366$12.00

1995]. Globally, shifts in carbon fluxes from C_3 and C_4 ecosystems on interannual and decadal timescales influence the $\delta^{13}C$ of atmospheric CO_2 and consequently the ways that this tracer is used for partitioning land and ocean carbon sources and sinks [*Ciais et al.*, 1999; *Townsend et al.*, 2002; *Still et al.*, 2003a].

[3] Recent analysis of trace gas measurements by *Langenfelds et al.* [2002] provide evidence that much of the global interannual variability of CO_2, CO, CH_4, and H_2 during the middle and late 1990s was caused by fires. Concurrent $\delta^{13}CO_2$ measurements from *Langenfelds et al.* [2002] suggest that origin of the emissions anomalies was burning in forests. This "C_3" isotopic signature is qualitatively consistent with reports of increased burning activity during the 1997/1998 El Niño event in closed canopy forests in South America [*Cochrane et al.*, 1999; *Nepstad et al.*, 1999], and tropical forests and peatlands in Southeast Asia [*Levine*, 1999; *Siegert et al.*, 2001; *Page et al.*, 2002]. However, it is likely that other processes contributed to the atmospheric $\delta^{13}CO_2$ anomalies during this period, including different sensitivities of net primary production (NPP) and heterotrophic respiration (R_h) to drought and temperature [e.g., *Jones and Cox*, 2001], the effect of El Niño-induced drought stress on the ratio of stomatal conductance to photosynthesis in tropical ecosystems [*Keeling et al.*, 2001; *Langenfelds et al.*, 2002; *Randerson et al.*, 2002a; *Scholze et al.*, 2003], and ocean exchange [*Feely et al.*, 1999]. As a result, some uncertainty remains as to whether fire emissions from C_4 grasslands increased in parallel to that observed in C_3 tropical forests during the 1997/1998 El Niño event, or if differences in regional climate or ecosystem processes led to a divergent emissions response between the two vegetation types.

[4] The availability of new satellite data products has made it possible to investigate patterns of C_3 and C_4 fire emissions at continental to global scales. Records of fire activity in the tropics extend from 1998 to the present from the Tropical Rainfall Measuring Mission (TRMM) Visible and InfraRed Spectrometer (VIRS) [*Giglio et al.*, 2000], and globally from mid-1996 to the present from the Along Track Scanning Radiometer (ATSR) [*Arino et al.*, 1999]. More recent satellite observations from the Moderate Resolution Imaging Spectroradiometer (MODIS) provide a means for converting these records of fire activity into time series of burned area [*Justice et al.*, 2002]. In addition, a contemporary global map of fractional C_4 canopy cover [*Still et al.*, 2003a] derived from other satellite and land cover sources [e.g., *DeFries et al.*, 2000] allows for a partitioning of NPP and burned area between C_3 and C_4 vegetation types.

[5] When combined, these satellite products allow us to explore hypotheses regarding the processes regulating fire emissions. In low productivity grasslands, for example, the effect of drought may have the opposite effect on fire activity from that in highly productive forest ecosystems. *Justice et al.* [1996] and *Barbosa et al.* [1999] provide evidence that drought in southern Africa decreases the extent of burned areas in xeric vegetation during the following dry season because anomalously low NPP limits fuel density, and thus the spread of fires. This negative feedback has also been recognized by the need for minimum net primary production (NPP) and aboveground biomass thresholds for fire activity in global prognostic fire models [*Thonicke et al.*, 2001]. It remains unknown what kind of effect this feedback may have on global CO_2 and $\delta^{13}CO_2$ levels or their interannual variability.

[6] Within savannas, fires play an important role in regulating the abundance of grasses and trees, along with other controls such as nutrient and water availability, and other forms of disturbance such as herbivory and grazing [*Medina and Silva*, 1990; *Scholes and Archer*, 1997]. Many studies have documented rapid, substantial increases in the population size and productivity of woody species over a period of years to decades following fire suppression [e.g., *Moreira*, 2000]. This rapid response may be partly attributed to decreases in the mortality rate of young saplings and woody shrubs growing within the grass layer [*Hoffmann and Moreira*, 2002]. Typically mortality rates for young trees are high because of the vulnerability of living tissue (leaves and woody stems) to ground fires, particularly during the dry season when the aboveground tissues of many grasses are senescent. In addition, frequent fires decrease litter and shading within the herbaceous layer, thus increasing the susceptibility of seedlings to mortality from drought stress [*Hoffmann*, 1996]. With increasing stature and age class, fire-induced tree mortality declines as a result of some combination of (1) the development of protective bark [*Gill*, 1981; *Gignoux et al.*, 1997], (2) greater belowground carbohydrate storage [*Gignoux et al.*, 1997], and (3) a decrease in fire damage to the canopy because of its increased height (thus separation from fuels in the surface layer) [*Shea et al.*, 1996]. This dynamic equilibrium between tree and grass plant functional types makes savanna carbon fluxes and their isotopic composition sensitive to shifts in the fire regime that occur in response to drought stress on ENSO (El Niño–Southern Oscillation) timescales, and in response to human pressures such as fuel wood collection and agriculture on decadal and century timescales [*Hao and Liu*, 1994; *Ramankutty and Foley*, 1999; *Ludwig et al.*, 2003; *Yevich and Logan*, 2003].

[7] The complexity of the ecological and socio-economic processes described above makes it challenging to isolate tree and grass contributions to fire emissions in savannas and at savanna-forest boundaries. Nevertheless, new modeling frameworks to achieve this partitioning are needed for an improved understanding of ecosystem functioning in response to multiple elements of global change, and more immediately, for the interpretation of variability in atmospheric trace gases, including CO_2, CO, and CH_4, and their isotopic variations. Here we present a first attempt, at a global scale, to estimate fire emissions from C_3 and C_4 vegetation using satellite data [*Arino et al.*, 1999; *Giglio et al.*, 2000], a global map of C_4 vegetation cover [*Still et al.*, 2003a], and a biogeochemical model [*Van der Werf et al.*, 2003, 2004]. Our objectives were to assess differences in climate and ecosystem controls on fire in C_3 and C_4 vegetation at interannual timescales and to improve our understanding and use of atmospheric $\delta^{13}CO_2$ as a tracer in atmospheric inversion studies of regional carbon sources and sinks. As a part of our analysis, we estimate the

contribution of fires to variability in global atmospheric $\delta^{13}CO_2$ during 1997–2001.

2. Methods

[8] In this section, we describe the fire emissions time series used in our study (section 2.1), the approach for estimating the C_3 and C_4 fractions of fire emissions in each grid cell (section 2.2), how we compared our model results with atmospheric data (section 2.3), and the techniques we used to study the mechanisms regulating interannual variability in fire emissions (section 2.4).

2.1. Fire Emissions

[9] In our analysis we used the CASA biogeochemical model with modifications for fire as described by *Van der Werf et al.* [2003, 2004]. A key feature of this modeling approach is that satellite data are used to constrain both the spatial distribution and timing of areas burned and the distribution of fuels. Total fire emissions reported here are the same as those from *Van der Werf et al.* [2004], although we made additional modifications to the model, described in section 2.2, to partition carbon fluxes in each grid cell to C_3 and C_4 vegetation types.

[10] A first step in generating this time series of fire emissions was to construct a continuous global time series of burned area. This was done by calibrating TRMM and ATSR satellite records of fire "hot spots" using MODIS-derived estimates of burned area. Where TRMM data were available (38°S to 38°N, over the period 1998–2001), we converted TRMM fire counts to burned area using a relationship that depended on the density of tree cover [*DeFries et al.*, 2000]. ATSR (algorithm 1) data allowed for the extension of our global burned area time series back in time by 1 year (to January 1997) and for the extension of spatial coverage to regions north of 38°N [*Van der Werf et al.*, 2004].

[11] Fuels are represented in the CASA model as aboveground and surface litter carbon pools, with inputs from NPP, allocation to wood based on fractional tree cover, and losses to fire, decomposition, herbivory, and fuel wood collection by humans. The model operates globally with a $1^\circ \times 1^\circ$ spatial resolution and a monthly time step. To capture interannual variability in ecosystem processes (NPP and decomposition) during the 1997 to 2001 period, we used available monthly data sets of Global Precipitation Climatology Project (GPCP) version 2 precipitation (http://precip.gsfc.nasa.gov) [*Huffman et al.*, 1997; *Susskind et al.*, 1997], air temperature anomalies [*Hansen et al.*, 1999], fraction of absorbed photosynthetically active radiation (FPAR) by green leaves, and burned area (described above). FPAR was derived from Advanced Very High Resolution Radiometer Normalized Difference Vegetation Index [*Los et al.*, 1994; *Tucker et al.*, 2005].

2.2. C_4 and C_3 Fire Emissions Methodology

[12] *Still et al.* [2003a] constructed a contemporary map of fractional C_4 canopy cover that accounts for the distribution of herbaceous and woody vegetation in the tropics [*DeFries et al.*, 2000], for C_3 and C_4 crops, and for mixed C_4 and C_3 grasslands in temperate regions where climate conditions are favorable for C_4 photosynthesis only during parts of the growing season. We used this map with the CASA biogeochemistry model to track separately C_3 and C_4 carbon pools and fluxes, including aboveground biomass and soil carbon pools, NPP, and fire emissions.

[13] C_4 NPP and burned area in grid cells with mixed C_3 and C_4 canopies were assumed to be proportional to the C_4 fractional canopy cover map. The entire C_4 fraction of a grid cell was assumed to consist of herbaceous vegetation with a 1:1 allocation of NPP to leaves and fine roots. In contrast, C_3 vegetation often had both herbaceous and woody components [*Still et al.*, 2003a]. The herbaceous component of C_3 vegetation was also assigned a 1:1 allocation of NPP to leaves and fine roots, whereas the woody component of C_3 vegetation had 1:1:1 allocation of NPP to leaves, stems, and fine roots.

[14] Biomass burning of agricultural waste and fuel wood [e.g., *Yevich and Logan*, 2003] are included within our modeling framework in a simple way. Fuel wood for cooking is removed from the coarse woody debris pool in each grid according to human population size and a per capita fuel wood use [*Van der Werf et al.*, 2003]. This flux was assumed to be uniform from month to month during 1997–2001 and was not included in the fire emission fluxes reported here. In contrast, agricultural waste burning that occurred in fields was captured, at least partially, by both our burned area algorithm and our C4 map, and so it was included as a part our emissions estimates presented here. Where United Nations Food and Agricultural Organization data on crop type were available, *Still et al.* [2003a] partitioned crops from *Ramankutty and Foley* [1999] into C3 and C4 components.

[15] The combined modifications to the biochemistry and diffusive pathways for CO_2 within the leaves of C_4 plants decrease levels of ^{13}C discrimination (approximately 4‰) as compared with that found in C_3 plants (approximately 19‰) [*Farquhar et al.*, 1989]. These differences in discrimination lead to comparable offsets in the $\delta^{13}C$ of plant tissues: isotopic surveys of leaves of contemporary C_3 and C_4 plant species show that the $\delta^{13}C$ of C_4 plants ranges between −9‰ and −16‰ [*Cerling et al.*, 1997; *Cerling*, 1999], whereas the $\delta^{13}C$ of C_3 plants range between −19‰ and −34‰ [*Körner et al.*, 1991; *Cerling et al.*, 1997; *Cerling*, 1999]. Although these ranges are broad, the $\delta^{13}C$ of most plants species and most aboveground biomass exhibits considerably less variability: between −11‰ and −13‰ for C_4 and between −25‰ and −30‰ for C_3 [*Körner et al.*, 1991; *Cerling et al.*, 1997]. Further, at ecosystem to biome scales, the range of $\delta^{13}C$ values of respiration from Keeling plots and atmospheric measurements appears far narrower than that reported for the isotopic composition of individual plant species [*Keeling et al.*, 2001; *Randerson et al.*, 2002b; *Miller et al.*, 2003; *Pataki et al.*, 2003; *Still et al.*, 2003b]. On the basis of these atmospheric studies, we assigned all C_4 vegetation a $\delta^{13}C$ of −12.5‰ and all C_3 vegetation a $\delta^{13}C$ of −27.5‰ for the 1997–2001 period. The sensitivity of our results to our choice of these C_3 and C_4 end-members is explored in an analysis at the end of section 3.1.

[16] Although there is considerable evidence that ^{13}C discrimination during photosynthesis shows substantial seasonal and interannual variability in C_3 ecosystems in response to climate [*Bowling et al.*, 2002; *Ometto et al.*, 2002; *Scholze et al.*, 2003], we did not attempt to take this into account in our analysis because we were interested in the $\delta^{13}C$ of fuels. In forests, wood, coarse woody debris, and litter pools contribute substantially fuel loads and all have mean ages of several years to several decades, effectively damping short-term variations caused by photosynthetic discrimination.

2.3. Fire Emissions Contributions to Atmospheric $\delta^{13}CO_2$

[17] The impact of fire emissions on interannual variability of atmospheric $\delta^{13}CO_2$ was estimated using the following approach. We converted the fire emissions time series (of total carbon) described above into CO_2 fluxes using emissions factors from *Andreae and Merlet* [2001] as described by *Van der Werf et al.* [2004]. We then used these CO_2 fluxes as the surface boundary condition for the GEOS-CHEM atmospheric chemistry model [*Bey et al.*, 2001], making a forward model run over the 1997–2001 period. In this analysis, the GEOS-CHEM model had a $4^\circ \times 5^\circ$ horizontal resolution and 30 vertical levels, and was driven using meteorological variables from NASA/DAO Data Assimilation System (DAS) for the year 2000. In the atmospheric model run, we separately tracked the space-time distribution of CO_2 concentrations arising from fire emissions from each of seven continental-scale regions. The atmospheric model was allowed to reach steady state over a 3-year period (using fire emissions from 2000 as the surface boundary condition) prior to the start of the interannual run. By carrying the seven separate tracers within the model, it was possible to identify the contribution of emissions from a particular source region to a CO_2 concentration anomaly recorded at a flask station [*Van der Werf et al.*, 2004].

[18] We then assigned a single $\delta^{13}C$ value to each of the seven CO_2 time series (tracers) within the GEOS-CHEM model. Concentration anomalies of CO_2 in the atmospheric model were converted to atmospheric $\delta^{13}CO_2$ anomalies by assuming that the fire emissions represented a small, linear perturbation to a mean background atmosphere during 1997–2001 comprised of 368 ppm CO_2 and a $\delta^{13}CO_2$ of -7.9‰. With this background atmosphere, a CO_2 increase arising solely from C_3 vegetation decreases atmospheric $\delta^{13}CO_2$ by -0.0531‰/ppm, whereas a CO_2 increase arising solely from C_4 vegetation decreases $\delta^{13}CO_2$ by only -0.0125‰/ppm.

[19] The fraction of emission anomalies arising from C_4 vegetation during 1997–2001 was computed using the following equation:

$$C_4 fract(i) = \frac{\sqrt{\sum_{t=1}^{60} C_4 anom(t,i)^2}}{\sqrt{\sum_{t=1}^{60} C_4 anom(t,i)^2} + \sqrt{\sum_{t=1}^{60} C_3 anom(t,i)^2}}, \quad (1)$$

where t is the monthly time step (from January 1997 to December 2001), i is the continental-scale source region, and $C_4 anom$ and $C_3 anom$ were constructed by first removing a mean seasonal cycle from the C_3 or C_4 fire emissions time series in each region.

[20] We converted each CO_2 tracer (one from each of the seven continental-scale source regions) to atmospheric $\delta^{13}CO_2$ using a separate value in each region,

$$S(i) = -0.0125 - 0.0406 \cdot (1 - C_4\, fract(i)), \quad (2)$$

where $S(i)$ had units of ‰/ppm and the slope and offset of equation (2) were determined using the isotopic values assigned to C_3 and C_4 vegetation (-27.5‰ and -12.5‰, respectively, as described in section 2.2) and the mass and isotopic composition of CO_2 in the mean background atmosphere described above (368 ppm and -7.9‰).

[21] The modeling approach described above, in which fire emissions from a biogeochemical model were used as input to the atmospheric transport model, will be hereinafter referred to as the forward model. We also report the impact of fire emissions on atmospheric $\delta^{13}CO_2$ using the CO_2 tracers from *Van der Werf et al.* [2004] that were adjusted using a single scalar in each continental-scale region to bring into agreement model predictions and observations of atmospheric CO anomalies during 1997–2001. This inversion procedure considerably amplified the magnitude of fire emissions anomalies from several regions dominated by C_3 vegetation, including Southeast Asia, and as a result, the inversion-constrained emissions time series presented here also have a larger impact on atmospheric $\delta^{13}CO_2$ anomalies than the forward model. The approach of using fire emissions constrained from an atmospheric CO inversion will be hereinafter referred to as the inversion-adjusted model. We compared our model estimates with atmospheric $\delta^{13}CO_2$ and CO_2 observations from the NOAA/CMDL flask network [*Trolier et al.*, 1996; *Miller et al.*, 2003].

2.4. Analysis Approaches

[22] To help understand how interannual fire emissions varied as a function of vegetation type, we partitioned fire emissions along a moisture gradient in regions within the TRMM footprint (between 38°N and 38°S). The different vegetation classes were defined according to mean annual precipitation (MAP; from GPCP v2) and percent tree cover [*DeFries et al.*, 2000], following the approach described by *Van der Werf et al.* [2003]. Closed canopy broadleaf forest was defined as MAP greater than 1500 mm/yr and percent tree cover greater than 85%, open canopy moist woodland was defined as MAP greater than 1500 mm/yr and percent tree cover less than 85%, intermediate woodland was defined as MAP between 1500 mm/yr and 1000 mm/yr, grasses with shrubs was defined as MAP between 1000 mm/yr and 500 mm/yr, and grasses, shrubs, and deserts was defined as MAP less than 500 mm/yr.

[23] To explore the vulnerability of tropical ecosystems to fire during periods before the TRMM and ATSR satellite era, we constructed a moisture threshold using TRMM fire counts and monthly precipitation observations. A moisture index, $M(t)$, was defined in a simple way using a weighted

Table 1. Fire Emissions From C_3 and C_4 Ecosystems (1997–2001)

	Time Period					
	1997	1998	1999	2000	2001	Mean 1997–2001
C_3 emissions, Pg C/yr	2.6	3.2	2.3	2.0	2.1	2.5
C_4 emissions, Pg C/yr	0.9	1.2	1.1	1.1	1.0	1.1
Emissions $\delta^{13}C$, ‰	−23.5	−23.4	−22.8	−22.2	−22.6	−22.9
C_4 emissions fraction	0.27	0.28	0.31	0.35	0.32	0.31

mean of GPCP v2 monthly precipitation, P, from the current month and the previous 3 months,

$$M(t) = 0.1 \times P(t-3) + 0.2 \times P(t-2) + 0.3 \cdot P(t-1) + 0.4 \times P(t). \quad (3)$$

Using concurrent TRMM fire count data, we established a threshold of this moisture index below which fire activity was no longer inhibited by moisture levels. We set this threshold as the value of the moisture index (100 mm/month) that corresponded to the ninetieth percentile of TRMM fire counts (distributed as a function of increasing *M*) from areas with over 1000 mm of mean annual precipitation. With this threshold established from TRMM data from 1998–2001, we then examined the fraction of tropical biomes that were vulnerable to fire during 1981–2001 (the time period when GPCP v2 data were available). In a separate analysis, on the dry end of the moisture gradient, we investigated links between precipitation and fire activity by comparing satellite-derived estimates of burned area with precipitation observations from northern Australia.

3. Results

3.1. C_3 and C_4 Fire Emissions During 1997–2001

[24] Using our approach, C_4 vegetation accounted for 31% of fire carbon emissions (Table 1) and 57% of the burned area during 1997–2001. The mean $\delta^{13}C$ of fire emissions was −22.9‰, based on the C_4 fraction of emissions described above and the assigned C_3 and C_4 isotopic end-members described in section 2.2. Globally, about 23% of carbon in C_4 aboveground biomass was lost via fire emissions each year (1.1 Pg C/yr out of a total aboveground biomass of 4.7 Pg C) as compared to 0.6% in C_3 vegetation (2.5 Pg C/yr out of a total of 444 Pg C). C_4 vegetation contributed to 20% (11 Pg C/yr) of global mean annual NPP (56 Pg C/yr).

[25] During the 1997/1998 El Niño event, fire emissions peaked during two distinct periods (August through November of 1997 and March through August of 1998) that roughly coincided with large deficits in tropical precipitation (Figure 1). During the first period, the positive emissions anomaly was entirely C_3 in origin, whereas during the second period, anomalously high emissions occurred in both C_3 and C_4 vegetation types (Figure 1b). Global fire emissions were lowest during 2000, primarily as a result of decreased C_3 emissions, and coincided with consistently high positive precipitation anomalies in both C_3 and C_4 vegetation throughout the year (Table 1, Figure 1). Annually, when global fire emissions were at a maximum in 1998, the C_4 fraction of global emissions was 0.28 (Table 1). When global fire emissions were at a minimum in 2000, the C_4 fraction of emissions was at a maximum of 0.35.

[26] Overall, C_3 vegetation accounted for a greater fraction of the month-to-month and year-to-year variability of fire emissions, as compared with C_4 vegetation (Figure 1 and Table 2). Although C_4 ecosystems contributed to 31% of mean annual emissions at a global level, they accounted for only 24% of the emissions anomalies during 1997–2001, defined according to equation (1) (Table 2). As a result, the $\delta^{13}C$ of fire emissions anomalies during 1997–2001 was −23.9‰, according to equation (1) and the $\delta^{13}C$ end-members for C_3 and C_4 vegetation.

[27] Four tropical regions that contributed to increased fire emissions during the 1997/1998 El Niño were Southeast Asia, Central America and northern South America

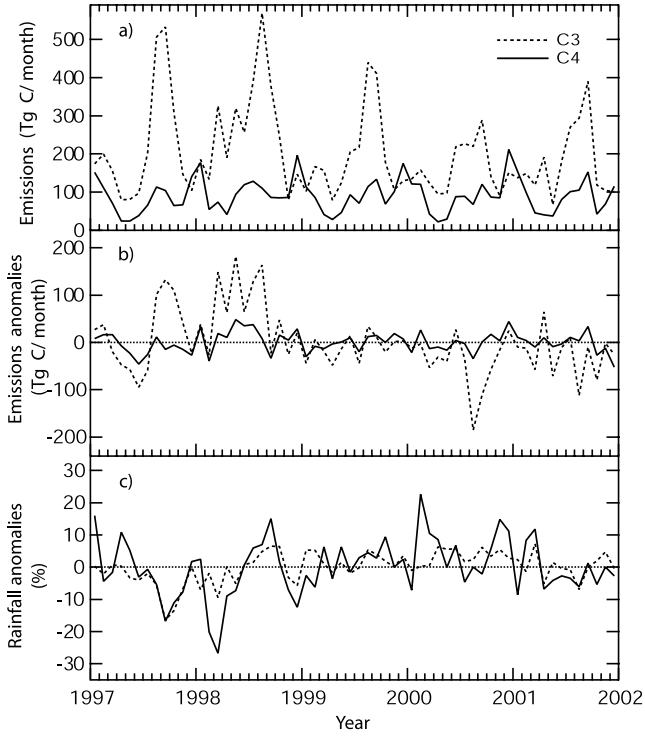

Figure 1. (a) Monthly global C_3 and C_4 fire emissions during 1997–2001. (b) C_3 and C_4 emissions anomalies after removing a mean seasonal cycle. (c) Precipitation anomalies over regions with C_3 and C_4 vegetation estimated from Global Precipitation Climatology Project (GPCP) version 2 monthly gridded observations. The precipitation anomalies were calculated using a spatial map of mean annual NPP to weight the observations across the land surface, and by fractionally attributing the anomalies in each grid cell using a C_3 or C_4 fractional canopy cover map [*Still et al.*, 2003a].

Table 2. Fire Emissions by Continental Region

Region	Mean Emissions, Tg C/yr	Mean C_4 Emissions,%	Mean% Tree Cover of Area Burned[a]	C_4 emissions Anomalies (equation (1)),%	El Niño[b] Emissions, Tg C	El Niño[b] C_4 Emissions,%	El Niño[b] % Tree Cover of Area Burned	La Niña Emissions, Tg C	La Niña C_4 Emissions,%	La Niña % Tree Cover of Area Burned
Southeast Asia	372	12	23	8	774	8	29	326	16	21
Central America and northern South America[c]	270	25	21	16	515	19	25	248	29	20
Southern South America	795	17	28	14	1022	14	30	522	17	26
Southern Africa	1015	33	26	34	1314	35	25	966	31	25
Northern Africa	802	56	15	50	676	58	16	811	57	15
Boreal[d]	142	0	23	0	152	0	21	109	0	17
Other[e]	134	56	10	64	131	55	10	158	56	7
Global	3530	31	21	24	4584	27	22	3141	33	19

[a]This index was constructed by averaging the percent tree cover from *DeFries et al.* [2000] within areas that burned during each time period.
[b]The El Niño period was defined as August 1997 through July 1998 and corresponded to a period when the mean SOI was negative. The La Niña period was defined as August 2000 through July 2001 and corresponded to a period when the mean SOI was positive. At the end of both periods, there was a period of several months when the SOI had a sign opposite to that of the mean.
[c]South America and Africa were divided into separate regions at the equator.
[d]Boreal consisted of all regions north of 38°N.
[e]Other regions included Australia, Central Asia, and the United States.

(north of the equator), southern South America (south of the equator), and southern Africa. During the El Niño, all of these regions experienced drought (Figure 2). In all of these regions, except southern Africa, the fraction of fire emissions from C_4 vegetation decreased during the El Niño (Figure 2) and was accompanied by a shift in the distribution of burned area within each region to areas with higher percent tree cover (and thus to areas with more C_3 fuels; Table 2). The shift in burned area within each region was probably a result of several factors linked with the drought, including enhanced ignition of woody fuels (that take longer to dry) and negative feedbacks on emissions in grasslands as a result of decreased levels of NPP (and thus fuel loads). North Africa and a composite of other regions including Australia, Central Asia, and the United States had lower emissions during 1997 and 1998, somewhat counteracting the global trends. In regions north of 38°N, fire emissions during the summer of 1998 were anomalously high as a result of fires in eastern Siberia and Canada [*Amiro et al.*, 2001; *Conard et al.*, 2002]. These boreal fires had a major impact on atmospheric CO and CO_2 in the Northern Hemisphere [*Kasischke et al.*, 2005; *Spichtinger et al.*, 2004], and had a depleted isotopic signature as they occurred almost exclusively in C_3 vegetation (Table 2).

[28] The C_4 emissions anomalies listed in Table 2 were used to set the $\delta^{13}CO_2$ of tracers in the GEOS-CHEM atmospheric model. Using fire emissions estimates obtained directly from the biogeochemistry model (the forward model), we found that fires contributed to approximately 27% of the observed decrease in atmospheric $\delta^{13}CO_2$ from mid-1997 to the end of 1998, and to 61% of the observed variance during 1997–2001 (Figure 3). Using fire emission estimates optimized in a previous study to match atmospheric CO anomalies [*Van der Werf et al.*, 2004] (the inversion-adjusted model), fires contributed to approximately 57% of the decrease from mid-1997 to the end of 1998 and to 72% of the variance during 1997–2001.

[29] In a sensitivity analysis, we increased the $\delta^{13}C$ of the C_3 and C_4 end-members by 1‰ in separate model runs. Changing the C_3 end-member (from −27.5‰ to −26.5‰) caused the $\delta^{13}C$ of global mean fire emissions to increase from −22.9‰ to −22.2‰. This change also decreased the amount of the atmospheric $\delta^{13}C$ anomaly during 1997/1998 attributable to fires. With the inversion-adjusted model, for example, the fire contribution to the 1997/1998 atmospheric $\delta^{13}C$ anomaly decreased from 57% to 54%. Increasing the $\delta^{13}C$ of the C_4 end-member had a similar effect on the directionality of both the isotopic composition of global mean fire emissions and the fire contribution to the atmospheric $\delta^{13}C$ anomaly, but with a smaller magnitude. The effect of end-member choice on the fire contribution to atmospheric $\delta^{13}C$ is small as compared with the differences between the forward biogeochemical and inversion-adjusted atmospheric model runs. This suggests that although the choice of the $\delta^{13}C$ end-members for C_3 and C_4 vegetation is important, it is our understanding of other processes including burned area and combustion completeness of C_3 and C_4 fuels in tropical savannas and forests that currently limits

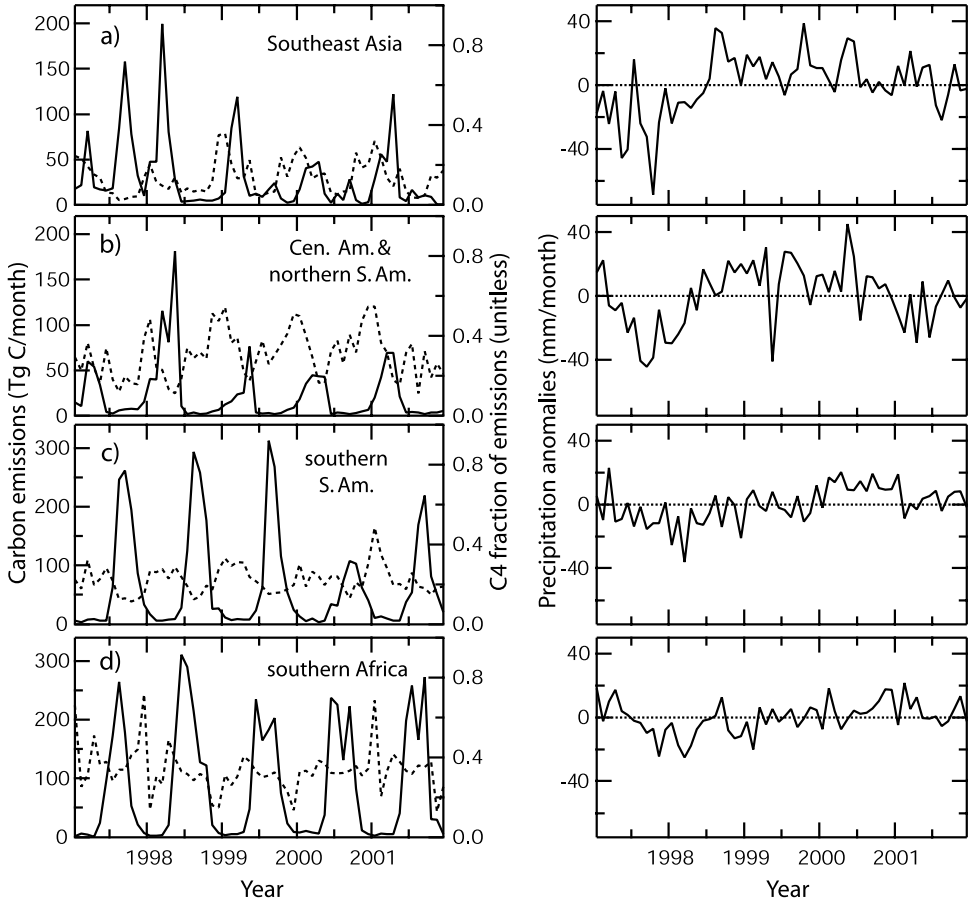

Figure 2. Fire emissions and the C_4 fraction of fire emissions from (a) Southeast Asia, (b) Central and northern South America, (c) southern South America, and (d) southern Africa. Fire emissions (left panel, left axis, solid line) are for total carbon and have units of Tg C/month. The C_4 fraction of fire emissions (left panel, right axis, dashed line) is unitless. Precipitation anomalies for each region (right panel, solid line) have units of mm/month. The precipitation anomalies were constructed by removing a mean seasonal cycle from 1997–2001 from each region.

our ability to estimate the fire contribution to atmospheric $\delta^{13}C$. These issues are explored in more detail in section 4.3.

3.2. Analysis of Mechanisms Responsible for C_3 and C_4 Emissions Variability

[30] To assess the relative importance of the mechanisms contributing to C_3 and C_4 emissions variability, we present additional results, including a biome-level partitioning of emissions along a moisture gradient, an analysis of the vulnerability of tropical biomes to fire during 1981–2001, and a time series of burned area from a low-precipitation region that may have experienced negative feedbacks on fire emissions from drought.

3.2.1. Variability in Fire Emissions Along a Moisture Gradient

[31] Partitioning regions by precipitation regime confirmed that much of the increase in fire emissions during 1997 and 1998 occurred in regions with high mean annual precipitation, high productivity, large stocks of aboveground biomass, and low percentages of mean annual C_4 NPP and C_4 biomass (biomes 1, 2, and 3 in Tables 3 and 4). Regions with low mean annual precipitation, NPP, and aboveground biomass (biome 5) had the opposite interannual pattern of fire emissions, with negative anomalies during 1997 and 1998, and positive anomalies during 2000.

3.2.2. Vulnerability of Tropical Ecosystems to Fire During 1981–2001

[32] We assessed the fraction of moist tropical biomes that were susceptible to burning between 1981 and 2001 using TRMM fire counts to identify a minimum level of moisture required to permit ignition and fire activity (Figure 4; see section 2.4). Over this 20-year period, the 1997/1998 El Niño stands out as the period when the greatest fraction of tropical forests and woodlands were susceptible to fires (Figure 5). In September of 1997, moisture levels were so low that they would have permitted fires in over 64% of closed canopy broadleaf forests (biome 1 in Table 3). In contrast, 2000 stands out as the year when the smallest fraction of closed canopy broadleaf forests were susceptible to fires during this 20-year record. Other periods of high fire

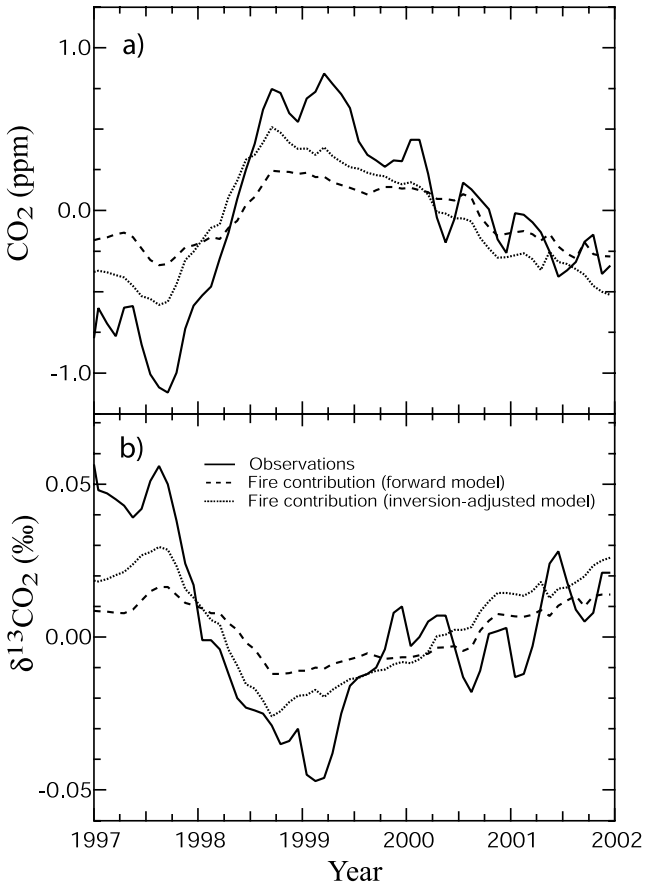

Figure 3. Atmospheric (a) CO_2 concentration and (b) $\delta^{13}CO_2$ anomalies during 1997–2001. Observations from the NOAA Climate Monitoring and Diagnostics Laboratory flask network are shown with the solid line, while modeled contributions from fire emissions are shown with dashed or dotted lines. Estimates of fire emissions directly from the forward biogeochemical model and the GEOS-CHEM atmospheric model are shown with the dashed line. Adjustments to the fire emissions from a CO inversion [*Van der Werf et al.*, 2004] are shown with the dotted line. The observed time series was constructed by removing a seasonal cycle from each flask station, and then subtracting a linear trend. The resulting anomalies at each station were averaged together within six latitude zones that were then area weighted to obtain the global time series shown here. The modeled fire contributions were constructed by sampling the atmospheric model in the same way as the observations.

vulnerability included 1982/1983, 1987, and 1991/1992, whereas periods of low fire vulnerability included 1989, 1990, and 1996. Open canopy woodlands (biome 2) had a similar but weaker series of trends (Figure 5b). More arid biomes (biomes 3 and 4) showed much less interannual variability in moisture inhibition of ignition and fire activity (Figures 5c and 5d). Biomes receiving fewer than 500 mm/yr of mean annual precipitation were rarely ignition limited, according to our threshold algorithm (section 2.4), and so they are not presented in Figure 5.

3.2.3. Drought, Fuel Loads, and Burned Area in Xeric Ecosystems

[33] On the xeric end of the moisture gradient, precipitation anomalies appeared to be positively correlated with burned area in some regions. For example, in northern Australia, precipitation and burned area anomalies were positively correlated during the 1997–2001 period (Figure 6) and were in phase with the Southern Oscillation Index (data not shown). Specifically, more area burned during a fire season following a wet growing season. In other xeric areas, however, precipitation and burned area was not correlated. Globally, precipitation anomalies in biome 5 (areas with fewer than 500 mm/yr mean annual precipitation) were at a minimum in 1998 and at a maximum in 2000, corresponding to the same 2 years as the minimum and maximum of fire emissions anomalies from this biome.

4. Discussion

4.1. Mechanisms

[34] Our analysis provides evidence that the increase in fire emissions during the 1997/1998 El Niño event occurred primarily in C_3 vegetation and thus had a depleted $\delta^{13}C$ signature. This finding is consistent with what was first inferred by *Langenfelds et al.* [2002] based on atmospheric $\delta^{13}CO_2$ observations and reports of increased burning during 1997 and 1998 in tropical forests of South America and Southeast Asia [*Nepstad et al.*, 1999; *Siegert et al.*, 2001; *Page et al.*, 2002]. The satellite-derived burned area data analyzed here provide evidence that global C_4 fire emissions did not increase in parallel during this event. More broadly, our model simulations (shown in Figure 3) contribute to an accumulating body of evidence that fire emissions from tropical forests drive much of the interannual variation of atmospheric CO_2 and $\delta^{13}CO_2$ [*Langenfelds et al.*, 2002; *Van der Werf et al.*, 2004]. During the 1997/1998 El Niño, widespread drought may have decreased levels of NPP and heterotrophic respiration in parallel, such that the net effect of these two processes had less impact on atmospheric $\delta^{13}CO_2$ than the concurrent increase in fire emissions.

[35] The primary mechanism for the depleted $\delta^{13}CO_2$ of fire emissions during the 1997/1998 El Niño appears to be linked with increased emissions from Southeast Asia, Central and South America, and boreal forests in the northern extratropics. Fire emissions from these areas increased substantially and were characterized by a high percentage of mean annual C3 emissions. Further, during the El Niño-induced drought, fires within Southeast Asia and Central and South America shifted into areas with more abundant tree cover (Figure 2, Table 2).

[36] Multiple economic factors in these tropical regions are causing net deforestation [*Achard et al.*, 2002; *Houghton*, 2003]. Fire is a key tool in the land clearing process [*Nepstad et al.*, 1999; *Page et al.*, 2002; *Cochrane*, 2003; *Achard et al.*, 2004], and our analysis suggests that human use of fire was strongly modulated by ENSO during

Table 3. Vegetation Properties Along a Moisture Gradient

Biome Number, Description	Rainfall Limits, mm/yr	Tree Cover Range,[a] %	Total Area, $\times 10^{12}$ m^2	Annual Mean Rainfall, mm/yr	NPP, g C/m^2/yr	C_4 NPP Fraction, %	Aboveground Biomass, kg C/m^2
1, closed canopy broadleaf forests	>1500	73–84	7.8	2086	1638	5	18.03
2, open canopy moist woodlands	>1500	14–64	12.0	1846	915	25	5.10
3, intermediate woodlands	1000–1500	10–54	15.5	1207	649	36	3.68
4, grasslands with shrubs	500–1000	1–41	15.3	794	403	42	1.74
5, grasslands, shrubs, and desert	<500	0–6	31.9	250	74	45	0.17
6, extratropics (north of 38°N)	no limit	0–57	49.2	574	286	4	3.15

[a]Values given are the tenth and ninetieth percentiles.

1997–2001 at a global scale. It was enhanced by prolonged drought during the El Niño, and it was inhibited by above average levels of precipitation during the La Niña year of 2000 (Figure 1). This work suggests that future trajectories of land use change may be linked with the future intensity and frequency of ENSO, in addition to better recognized economic, social, and political drivers [e.g., *Curran et al.*, 2004].

[37] Negative feedbacks on C_4 emissions also probably contributed to reduced C_4 emissions during the 1997/1998 El Niño. In low productivity savanna regions that had a high percentage of mean C4 emissions (biome 5 in Table 4), total fire emissions were at a minimum during the 1997/1998 El Niño, and at a maximum during the La Niña wet spell in 2000. As such, this biome had the opposite pattern of interannual emissions as compared to biomes on the wet end of moisture gradient (biomes 1 and 2). There are two possible reasons for this. First, in some low productivity regions, drought stress associated with the El Niño may have limited NPP, fuel density, and thus the spread of fires. This appeared to be an important mechanism in northern Australia (Figure 6) and is consistent with previous satellite observations in southern Africa from the late 1980s and early 1990s [*Justice et al.*, 1996; *Barbosa et al.*, 1999] and with observations from fire scars on tree rings in the southwestern United States [*Swetnam and Betancourt*, 1998]. Second, perhaps because ENSO is a phenomena primarily centered in the equatorial Pacific, shifts in precipitation in many dry subtropical ecosystems, further removed from the equator, were generally weaker, and less coherent between years when globally aggregated during 1997–2001.

[38] While drought stress effects on NPP and fuel density in low productivity ecosystems may have limited C_4 emissions in some regions during the 1997/1998 El Niño, at the global scale this mechanism is of secondary importance in regulating atmospheric CO_2 and $\delta^{13}CO_2$ anomalies caused by fire. The reason is that the anomalies in fire emissions from these regions were a factor of 3–5 smaller than those from high productivity tropical forest, woodland, and moist savanna areas (dominated by C_3 vegetation), and a factor of 2 smaller than those from boreal forests, where C_4 plants are not a significant component of biomass (Table 4).

[39] A schematic representation of the response of global fire emissions to ENSO is given in Figure 7. Because of the substantial accumulation of woody fuels over a period of many decades in closed canopy forests and open canopy woodlands on the wet end of the tropical fire gradient, modulation of the moisture limits on ignition and fire activity by ENSO (Figure 5) has the potential to have a larger impact on atmospheric CO_2 fluxes than concurrent decreases in fire emissions at the xeric end of the moisture gradient. Considered together, concurrent shifts in the C_3 and C_4 fire regime during ENSO amplify year to year variations in the $\delta^{13}C$ of fire emissions and subsequently variations in atmospheric $\delta^{13}CO_2$.

4.2. The $\delta^{13}CO_2$ as an Integrator of CO_2, CO, CH_4, and H_2 Emissions Ratios

[40] The inverse approach of using atmosphere concentrations of multiple trace gas species to estimate total carbon emissions from fires requires reliable information on emissions ratios (such as CO:CO_2, CH_4:CO_2, and H_2:CO_2 ratios) [e.g., *Pak et al.*, 2003]. While numerous field and aircraft

Table 4. Fire Emissions Along a Moisture Gradient

Biome Number, Description	Fire Emissions, Tg C/yr	C_4 Fire Emissions Fraction, %	Emissions Anomalies During 1997–2001, Tg C/yr				
			1997	1998	1999	2000	2001
1, closed canopy broadleaf forest	132	1	119	43	−32	−69	−60
2, open canopy moist woodland	1088	22	240	296	−172	−232	−132
3, intermediate woodland	1434	36	−132	306	85	−182	−77
4, grassland with shrubs	655	46	−81	109	31	−24	−35
5, grassland, shrubs, and desert	77	69	−25	−1	0	22	4
6, extratropics	144	0	−83	196	−47	−9	−57

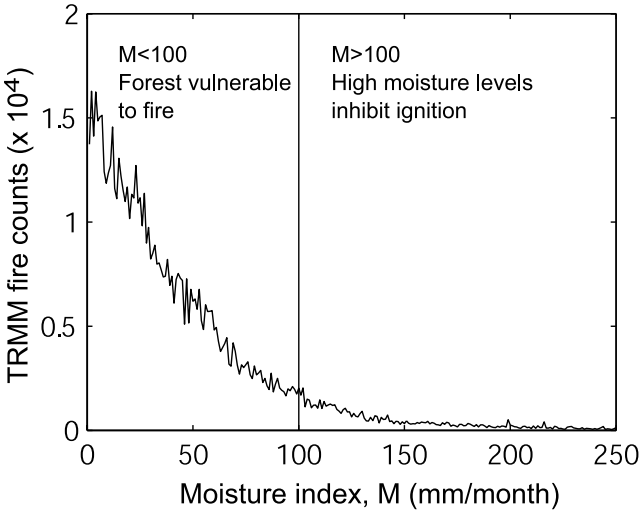

Figure 4. TRMM fire counts as a function of a moisture index, *M*, described in section 2.4. The fire counts and moisture index shown here were from tropical regions with mean annual precipitation greater than 1000 mm/yr (biomes 1, 2, and 3 in Table 3). Using this metric of fuel moisture, we found that 90% of all fire counts occurred below an *M* value of 100 mm/month during 1998–2001 (vertical solid line on graph). We define this value of the moisture index as a threshold for inhibition of fire activity by high levels of moisture. Vegetation is vulnerable to fire when *M* drops below this threshold ($M < 100$).

campaigns have provided detailed information on emission ratios, considerable uncertainty still remains as to their sensitivities to moisture levels, vegetation type, and fire intensity [*Andreae and Merlet*, 2001]. Satellite observations of fire activity provide critical "bottom up" constraints on emissions factors at regional and global scales by specifying the location and timing of fires and thus providing a link to additional information about local climate and fuel moisture levels, vegetation type (e.g., C_3 or C_4), and land use activities. In several respects, the $\delta^{13}CO_2$ associated with biomass burning plumes may serve as a useful integrator of the multiple processes that regulate emission factors for reduced gas species such as CO, CH_4, and H_2 across regions and continents.

[41] Specifically, the low surface area to volume ratio of stems, boles, and coarse woody debris fuels in woodlands and forests (C_3 pathway) may prolong the smoldering phase of emissions that favors the production of reduced trace gas species. In addition, many tropical forests have a closed canopy, which require longer periods of time to dry out, again enhancing the smoldering phase of emissions. Similarly, when humans use fire for land clearing purposes (that often occur in forests under moisture conditions suboptimal for fires) high levels of reduced gases may be produced. As a result, in tropical and subtropical regions, a depleted carbon isotope ratio of CO_2 in biomass burning plumes may be linked with more reduced gas production (and high values of emissions factors for reduced gases). In boreal regions the relationship between emission factors and the carbon isotope ratio may be the reverse of that in the tropics because severe fires lead to combustion of deeper, more isotopically enriched soil organic matter [*Schuur et al.*, 2003].

[42] The C_4 fractions and carbon isotope ratios that we estimate here for total carbon emissions are probably most applicable for CO_2 fluxes because CO_2 typically accounts for over 90% of total carbon emissions [*Andreae and Merlet*, 2001]. Since CO and CH_4 emissions are greatly enhanced during the smoldering phase of emissions and because woody fuels tend to promote smoldering phases of combustion [*Andreae and Merlet*, 2001], we would expect the C_4 fraction of emissions to be even smaller for these reduced gases than what we predicted here for CO_2. The isotopic composition of CH_4 is further modified during the combustion process, with the smoldering phase in wildfires leading to an isotopic depletion of CH_4 by several ‰ (relative to the starting fuels), while hot fires may lead to isotopic enrichment by several ‰ [*Chanton et al.*, 2000].

4.3. Reducing Uncertainties

[43] Estimating the carbon isotope ratio (and the total flux) of fire emissions requires accurate information on the distribution of burned area in savannas, woodlands, and tropical forests. Unfortunately, remote sensing estimates of burned area are particularly problematic in tropical woodlands and forests because fires are often small and because fires can be masked by tree cover and clouds. By

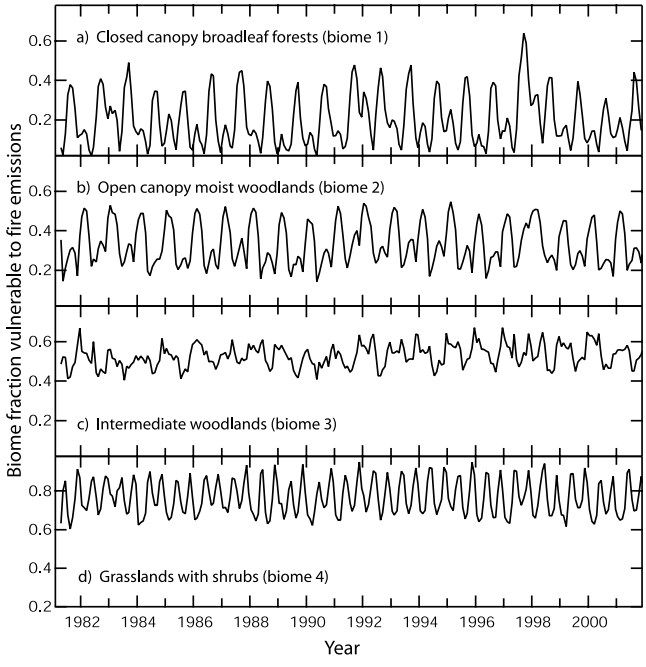

Figure 5. Fraction of each biome during the 1990 to 2001 period when moisture levels did not limit fire emissions. Moisture levels were assumed not to limit fire emissions when the moisture index described in Figure 4 was less than 100 mm ($M < 100$). The biomes are defined in Table 3 and section 2.4. Precipitation levels in each grid cell used to construct *M* were from GPCP v2 observations.

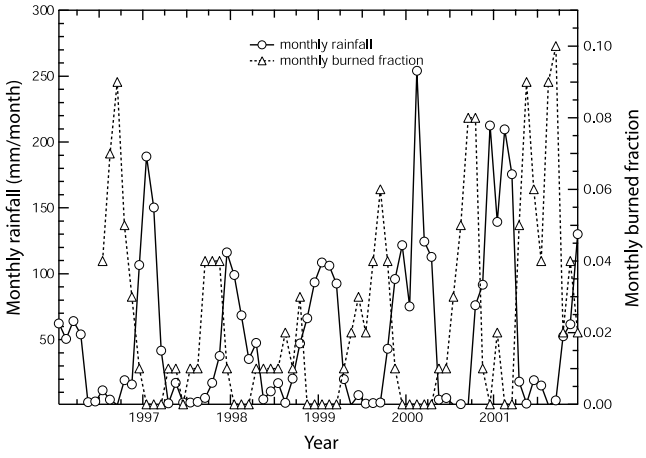

Figure 6. Precipitation anomalies (mm/month) and monthly burned area fraction (unitless) in Australia's Northern Territory during 1996–2001. This region spans latitudes between 26°S and 15°S and longitudes between 129°E and 128°E. Mean annual precipitation over this region was 645 mm/year. Rainfall during the wet season (from September to August) was significantly correlated with burned area during the following dry season (from January to December) ($r^2 = 0.86$, $p < 0.01$, $n = 5$). The slope of the linear relationship was 0.0072 ± 0.0002 with units of cumulative burned area fraction (during the dry season) per mm of wet season rainfall. The y intercept was -0.22 with units of cumulative burned area fraction (during the dry season). From 1998 through 2001 annual NDVI increased monotonically from 0.27 to 0.32, also showing a positive relationship with precipitation.

combining satellite data of different temporal and spatial resolutions with in situ studies of land use practices, considerable potential exists for improving our understanding of burned area over the next several decades in these biomes. Other factors contributing to uncertainties in a partitioning of C_3 and C_4 emissions include our limited understanding of fire-induced tree mortality, the combustion completeness of different grass and tree fuel types, and the balance between decomposition, fuel wood collection, fire, herbivory, and other forms of disturbance that regulate aboveground biomass levels and thus fuel loads. Both mortality and combustion completeness are closely linked with the type and purpose of the fire (e.g., deforestation, pasture maintenance, or lightning-set fires) as well as climate. While multiple data sources can be used to constrain the various processes that regulate fuel loads, much less is known at regional scales about relationships between fire severity, fire-induced tree mortality, and burned area and how these relationships change within different savanna and woodland ecosystems.

[44] A key assumption in our use of remote sensing data products was that the partitioning of burned area between herbaceous and woody vegetation at the $1^\circ \times 1^\circ$ spatial resolution of our model was proportional to the fractional cover of these two vegetation types averaged within the grid cell. With the future availability of high resolution burned area products from MODIS [*Justice et al.*, 2002], it will be possible to test the validity of this assumption and to check the degree to which the partitioning of burned area between herbaceous and woody areas depends on the resolution of the satellite data.

[45] In terms of assessing the impact of fire emissions on atmospheric $\delta^{13}C$, a key assumption that we made was that the $\delta^{13}C$ of fire emission anomalies within each region was constant over the 1997–2001 period (following equation (1) and Table 2). While we believe this approximation captured most of the variability over this period in this initial analysis, in future work we plan to allow fire emissions to have temporally varying C_3 and C_4 components throughout the duration of the atmospheric transport model run. Other key improvements will include using observational and modeling constraints to allow for the $\delta^{13}C$ of C_3 aboveground biomass to vary spatially with climate and land use

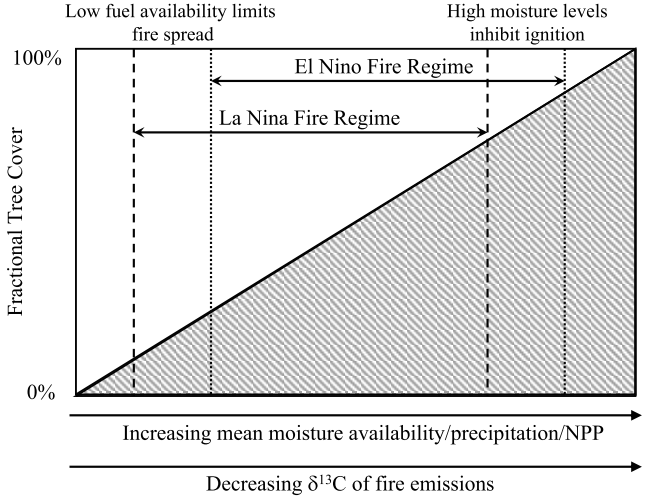

Figure 7. A conceptual model of shifts in the tropical fire regime during ENSO cycles. Vertical lines represent limits to fire emissions during El Niño (dotted line) and La Niña (dashed line) periods. The shaded wedge represents how the fraction of tree cover (y axis) varies across the moisture gradient (x axis). Fire emissions in areas with low mean annual precipitation (MAP) are limited by fuel loads (and thus NPP) and not by high levels of moisture that limit ignition. The opposite occurs in areas with high MAP. In areas with high MAP, El Niño-induced drought stress dries woody fuels and allows humans to more effectively use fire as a tool for land clearing. The isotopic signature associated with fire emissions during the El Niño is relatively depleted because of increased burning in areas with high fractional tree cover (tropical forests) and, secondarily, because of decreased burning in areas with low fractional tree cover (C4 grasslands) as a consequence of drought reducing C4 fuel loads. La Niña wet spells reduce fire frequency in tropical forests while increasing fuel availability and thus fire emissions from ecosystems dominated by C_4 grasses. As a result, fire emissions during La Niña have a relatively enriched isotopic signature, reflecting a greater contribution from C_4 grasses.

patterns [e.g., *Lloyd and Farquhar*, 1994; *Kaplan et al.*, 2002].

5. Conclusions

[46] C_4 ecosystems account for ~4% of contemporary global plant biomass [*Still et al.*, 2003a] and 20% to 27% of global primary production [*Lloyd and Farquhar*, 1994; *Fung et al.*, 1997; *Still et al.*, 2003a]. Building on these studies, we estimate that 31% of global fire emissions have a C_4 origin and that approximately one fifth of C_4 aboveground biomass returns to the atmosphere each year by fire. These satellite-derived estimates of global C_4 emissions highlight the importance of fire as a major biogeochemical and evolutionary force in savanna ecosystems.

[47] Most of the interannual variation in global fire emissions during the 1997 to 2001 period occurred in areas dominated by C_3 vegetation. For this reason, the $\delta^{13}C$ of global fire emissions anomalies was highly depleted, with a mean of −23.9‰. During the 1997/1998 El Niño, the first anomalously high emissions event in August through November of 1997 was almost entirely C_3 in origin, while the second emissions event in the middle of 1998 had a large C_3 and small C_4 component. As a consequence of the depleted $\delta^{13}C$ signature of emissions (and the large increase in total emissions), fires contributed substantially to the decrease in atmospheric $\delta^{13}CO_2$ observed between mid-1997 and the end of 1998.

[48] **Acknowledgments.** This work was supported by a NASA grant to J. Randerson (NNG04GK49G), P. Kasibhatla (NAG5-9605), and E. Kasischke (NAG5-9440). We thank C. J. Tucker for providing the NDVI time series used in this analysis and S. Olsen for analysis.

References

Achard, F., H. D. Eva, H. J. Stibig, P. Mayaux, J. Gallego, T. Richards, and J. P. Malingreau (2002), Determination of deforestation rates of the world's humid tropical forests, *Science*, *297*(5583), 999–1002.

Achard, F., H. D. Eva, P. Mayaux, H. J. Stibig, and A. Belward (2004), Improved estimates of net carbon emissions from land cover change in the tropics for the 1990s, *Global Biogeochem. Cycles*, *18*, GB2008, doi:10.1029/2003GB002142.

Amiro, B. D., J. B. Todd, B. M. Wotton, K. A. Logan, M. D. Flannigan, B. J. Stocks, J. A. Mason, D. L. Martell, and K. G. Hirsch (2001), Direct carbon emissions from Canadian forest fires, 1959–1999, *Can. J. For. Res.*, *31*(3), 512–525.

Andreae, M. O., and P. Merlet (2001), Emission of trace gases and aerosols from biomass burning, *Global Biogeochem. Cycles*, *15*(4), 955–966.

Arino, O., J.-M. Rosaz, and P. Goloub (1999), The ATSR World Fire Atlas: A synergy with "POLDER" aerosol products, *Earth Obs. Q.*, *64*, 1–6.

Barbosa, P. M., D. Stroppiana, J. M. Gregoire, and J. M. C. Pereira (1999), An assessment of vegetation fire in Africa (1981–1991): Burned areas, burned biomass, and atmospheric emissions, *Global Biogeochem. Cycles*, *13*(4), 933–950.

Bey, I., D. J. Jacob, R. M. Yantosca, J. A. Logan, B. D. Field, A. M. Fiore, Q. B. Li, H. G. Y. Liu, L. J. Mickley, and M. G. Schultz (2001), Global modeling of tropospheric chemistry with assimilated meteorology: Model description and evaluation, *J. Geophys. Res.*, *106*(D19), 23,073–23,095.

Bowling, D. R., N. G. McDowell, B. J. Bond, B. E. Law, and J. R. Ehleringer (2002), C-13 content of ecosystem respiration is linked to precipitation and vapor pressure deficit, *Oecologia*, *131*, 113–124.

Cerling, T. E. (1999), Paleorecords of C4 plants and ecosystems, in *C4 Plant Biology*, edited by R. F. Sage and R. K. Monson, pp. 445–469, Elsevier, New York.

Cerling, T. E., J. M. Harris, B. J. MacFadden, M. G. Leakey, J. Quade, V. Eisenmann, and J. R. Ehleringer (1997), Global vegetation change through the Miocene/Pliocene boundary, *Nature*, *389*, 153–158.

Chanton, J. P., C. M. Rutkowski, C. C. Schwartz, D. E. Ward, and L. Boring (2000), Factors influencing the stable carbon isotopic signature of methane from combustion and biomass burning, *J. Geophys. Res.*, *105*(D2), 1867–1877.

Ciais, P., P. Friedlingstein, D. S. Schimel, and P. P. Tans (1999), A global calculation of the delta C-13 of soil respired carbon: Implications for the biospheric uptake of anthropogenic CO_2, *Global Biogeochem. Cycles*, *13*(2), 519–530.

Cochrane, M. A. (2003), Fire science for rainforests, *Nature*, *421*(6926), 913–919.

Cochrane, M. A., A. Alencar, M. D. Schulze, C. M. Souza, D. C. Nepstad, P. Lefebvre, and E. A. Davidson (1999), Positive feedbacks in the fire dynamic of closed canopy tropical forests, *Science*, *284*(5421), 1832–1835.

Conard, S. G., A. I. Sukhinin, B. J. Stocks, D. R. Cahoon, E. P. Davidenko, and G. A. Ivanova (2002), Determining effects of area burned and fire severity on carbon cycling and emissions in Siberia, *Clim. Change*, *55*(1–2), 197–211.

Curran, L. M., S. N. Trigg, A. K. McDonald, D. Astiani, Y. M. Hardiono, P. Siregar, I. Caniago, and E. Kasischke (2004), Lowland forest loss in protected areas of Indonesian Borneo, *Science*, *303*(5660), 1000–1003.

DeFries, R. S., M. C. Hansen, J. R. G. Townshend, A. C. Janetos, and T. R. Loveland (2000), A new global 1-km dataset of percentage tree cover derived from remote sensing, *Global Change Biol.*, *6*(2), 247–254.

Farquhar, G. D., J. R. Ehleringer, and K. T. Hubick (1989), Carbon isotope discrimination and photosynthesis, *Annu. Rev. Plant Physiol. Plant Mol. Biol.*, *40*, 503–537.

Feely, R. A., R. Wanninkhof, T. Takahashi, and P. Tans (1999), Influence of El Niño on the equatorial Pacific contribution to atmospheric CO_2 accumulation, *Nature*, *398*(6728), 597–601.

Fung, I. Y., et al. (1997), Carbon 13 exchanges between the atmosphere and biosphere, *Global Biogeochem. Cycles*, *11*(4), 507–533.

Giglio, L., J. D. Kendall, and C. J. Tucker (2000), Remote sensing of fires with the TRMM VIRS, *Int. J. Remote Sens.*, *21*(1), 203–207.

Gignoux, J., J. Clobert, and J. C. Menaut (1997), Alternative fire resistance strategies in savanna trees, *Oecologia*, *110*, 576–583.

Gill, A. M. (1981), Fire adaptive traits of vascular plants, in *Fire Regimes and Ecosystem Properties*, edited by H. A. Mooney et al., general technical report, pp. 208–230, U.S. Dep. of Agric. For. Sci., Washington, D. C.

Hansen, J., R. Ruedy, J. Glascoe, and M. Sato (1999), GISS analysis of surface temperature change, *J. Geophys. Res.*, *104*(D24), 30,997–31,022.

Hao, W. M., and M.-H. Liu (1994), Spatial and temporal distribution of biomass burning, *Global Biogeochem. Cycles*, *8*(4), 495–503.

Hoffmann, W. A. (1996), The effects of fire and cover on seedling establishment in a neotropical savanna, *J. Ecol.*, *84*(3), 383–393.

Hoffmann, W. A., and A. G. Moreira (2002), The role of fire in population dynamics of woody plants, in *The Cerrados of Brazil: Ecology and Natural History of a Neotropical Savanna*, edited by P. S. Oliveira and R. J. Marquis, pp. 159–177, Columbia Univ. Press, New York.

Houghton, R. A. (2003), Revised estimates of the annual net flux of carbon to the atmosphere from changes in land use and land management 1850–2000, *Tellus, Ser. B*, *55*(2), 378–390.

Huffman, G. J., R. F. Adler, P. Arkin, A. Chang, R. Ferraro, A. Gruber, J. Janowiak, A. McNab, B. Rudolf, and U. Schneider (1997), The Global Precipitation Climatology Project (GPCP) Combined Precipitation Dataset, *Bull. Am. Meteorol. Soc.*, *78*(1), 5–20.

Jones, C. D., and P. M. Cox (2001), Modeling the volcanic signal in the atmospheric CO_2 record, *Global Biogeochem. Cycles*, *15*(2), 453–465.

Justice, C. O., J. D. Kendall, P. R. Dowty, and R. J. Scholes (1996), Satellite remote sensing of fires during the SAFARI campaign using NOAA advanced very high resolution radiometer, *J. Geophys. Res.*, *101*(D19), 23,851–23,863.

Justice, C. O., L. Giglio, S. Korontzi, J. Owens, J. T. Morisette, D. Roy, J. Descloitres, S. Alleaume, F. Petitcolin, and Y. Kaufman (2002), The MODIS fire products, *Remote Sens. Environ.*, *83*(1–2), 244–262.

Kaplan, J. O., I. C. Prentice, and N. Buchmann (2002), The stable carbon isotope composition of the terrestrial biosphere: Modeling at scales from the leaf to the globe, *Global Biogeochem. Cycles*, *16*(4), 1060, doi:10.1029/2001GB001403.

Kasischke, E., E. J. Hyer, P. Novelli, L. Bruhwiler, N. H. F. French, A. I. Sukhinin, J. H. Hewson, and B. J. Stocks (2005), Influences of boreal fire emissions on Northern Hemisphere atmospheric carbon and carbon monoxide, *Global Biogeochem. Cycles*, *19*, GB1012, doi:10.1029/2004GB002300.

Keeling, C. D., S. C. Piper, R. B. Bacastow, M. Wahlen, T. P. Whorf, M. Heimann, and H. A. Meijer (2001), Exchanges of atmospheric CO_2 and $^{13}CO_2$ with the terrestrial biosphere and oceans from 1978 to 2000, *SIO Ref. 01-06*, 45 pp., Scripps Inst. of Oceanogr., San Diego, Calif.

Körner, C., G. D. Farquhar, and S. C. Wong (1991), Carbon isotope discrimination by plants follows latitudinal and altitudinal trends, *Oecologia*, *88*, 30–40.

Langenfelds, R. L., R. J. Francey, B. C. Pak, L. P. Steele, J. Lloyd, C. M. Trudinger, and C. E. Allison (2002), Interannual growth rate variations of atmospheric CO_2 and $\delta^{13}C$, H_2, CH_4, and CO between 1992 and 1999 linked to biomass burning, *Global Biogeochem. Cycles*, *16*(3), 1048, doi:10.1029/2001GB001466.

Levine, J. S. (1999), The 1997 fires in Kalimantan and Sumatra, Indonesia: Gaseous and particulate emissions, *Geophys. Res. Lett.*, *26*(7), 815–818.

Lloyd, J., and G. D. Farquhar (1994), ^{13}C discrimination during CO_2 assimilation by the terrestrial biosphere, *Oecologia*, *99*, 201–215.

Los, S. O., C. O. Justice, and C. J. Tucker (1994), A global $1° \times 1°$ NDVI data set for climate studies derived from GIMMS continental NDVI data, *Int. J. Remote Sens.*, *15*(17), 3493–3518.

Ludwig, J., L. T. Marufu, B. Huber, M. O. Andreae, and G. Helas (2003), Domestic combustion of biomass fuels in developing countries: A major source of atmospheric pollutants, *J. Atmos. Chem.*, *44*, 23–37.

Martin, A., A. Mariotti, J. Balesdent, P. Lavelle, and R. Vuattoux (1990), Estimate of organic-matter turnover rate in a savanna soil by C-13 natural abundance measurements, *Soil Biol. Biochem.*, *22*(4), 517–523.

Medina, E., and J. F. Silva (1990), Savannas of northern South-America—A steady-state regulated by water-fire interactions on a background of low nutrient availability, *J. Biogeogr.*, *17*(4–5), 403–413.

Miller, J. B., P. P. Tans, J. W. C. White, T. J. Conway, and B. W. Vaughn (2003), The atmospheric signal of terrestrial carbon isotopic discrimination and its implication for partitioning carbon fluxes, *Tellus, Ser. B*, *55*(2), 197–206.

Moreira, A. G. (2000), Effects of fire protection on savanna structure in Central Brazil, *J. Biogeogr.*, *27*(4), 1021–1029.

Nepstad, D. C., et al. (1999), Large-scale impoverishment of Amazonian forests by logging and fire, *Nature*, *398*(6727), 505–508.

Ometto, J. P. H. B., L. B. Flanagan, L. A. Martinelli, M. Z. Moreira, N. Higuchi, and J. R. Ehleringer (2002), Carbon isotope discrimination in forest and pasture ecosystems of the Amazon Basin, Brazil, *Global Biogeochem. Cycles*, *16*(4), 1109, doi:10.1029/2001GB001462.

Page, S. E., F. Siegert, J. O. Rieley, H. D. V. Boehm, A. Jaya, and S. Limin (2002), The amount of carbon released from peat and forest fires in Indonesia during 1997, *Nature*, *420*(6911), 61–65.

Pak, B. C., et al. (2003), Measurements of biomass burning influences in the troposphere over southeast Australia during the SAFARI 2000 dry season campaign, *J. Geophys. Res.*, *108*(D13), 8480, doi:10.1029/2002JD002343.

Pataki, D. E., J. R. Ehleringer, L. B. Flanagan, D. Yakir, D. R. Bowling, C. J. Still, N. Buchmann, J. O. Kaplan, and J. A. Berry (2003), The application and interpretation of Keeling plots in terrestrial carbon cycle research, *Global Biogeochem. Cycles*, *17*(1), 1022, doi:10.1029/2001GB001850.

Ramankutty, N., and J. A. Foley (1999), Estimating historical changes in global land cover: Croplands from 1700 to 1992, *Global Biogeochem. Cycles*, *13*(4), 997–1027.

Randerson, J. T., G. J. Collatz, J. E. Fessenden, A. D. Munoz, C. J. Still, J. A. Berry, I. Y. Fung, N. Suits, and A. S. Denning (2002a), A possible global covariance between terrestrial gross primary production and ^{13}C discrimination: Consequences for the atmospheric ^{13}C budget and its response to ENSO, *Global Biogeochem. Cycles*, *16*(4), 1136, doi:10.1029/2001GB001845.

Randerson, J. T., et al. (2002b), Carbon isotope discrimination of arctic and boreal biomes inferred from remote atmospheric measurements and a biosphere-atmosphere model, *Global Biogeochem. Cycles*, *16*(3), 1028, doi:10.1029/2001GB001435.

Sage, R. F., and R. K. Monson (1999), *C4 Plant Biology*, 596 pp., Elsevier, New York.

Scholes, R. J., and S. R. Archer (1997), Tree-grass interactions in savannas, *Annu. Rev. Ecol. Syst.*, *28*, 517–544.

Scholze, M., J. O. Kaplan, W. Knorr, and M. Heimann (2003), Climate and interannual variability of the atmosphere-biosphere (CO_2)-C-13 flux, *Geophys. Res. Lett.*, *30*(2), 1097, doi:10.1029/2002GL015631.

Schuur, E. A. G., S. E. Trumbore, M. C. Mack, and J. W. Harden (2003), Isotopic composition of carbon dioxide from a boreal forest fire: Inferring carbon loss from measurements and modeling, *Global Biogeochem. Cycles*, *17*(1), 1001, doi:10.1029/2001GB001840.

Shea, R. W., B. W. Shea, J. B. Kauffman, D. E. Ward, C. I. Haskins, and M. C. Scholes (1996), Fuel biomass and combustion factors associated with fires in savanna ecosystems of South Africa and Zambia, *J. Geophys. Res.*, *101*(D19), 23,551–23,568.

Siegert, F., G. Ruecker, A. Hinrichs, and A. A. Hoffmann (2001), Increased damage from fires in logged forests during droughts caused by El Niño, *Nature*, *414*(6862), 437–440.

Spichtinger, N., R. Damoah, S. Eckhardt, C. Forster, P. James, S. Beirle, T. Wagner, P. C. Novelli, and A. Stohl (2004), Boreal forest fires in 1997 and 1998: A seasonal comparison using transport model simulations and measurement data, *Atmos. Chem. Phys. Discuss.*, *4*, 2747–2779.

Still, C. J., J. A. Berry, G. J. Collatz, and R. S. DeFries (2003a), Global distribution of C_3 and C_4 vegetation: Carbon cycle implications, *Global Biogeochem. Cycles*, *17*(1), 1006, doi:10.1029/2001GB001807.

Still, C. J., J. A. Berry, M. Ribas-Carbo, and B. R. Helliker (2003b), The contribution of C-3 and C-4 plants to the carbon cycle of a tallgrass prairie: An isotopic approach, *Oecologia*, *136*, 347–359.

Susskind, J., P. Piraino, L. Rokke, T. Iredell, and A. Mehta (1997), Characteristics of the TOVS Pathfinder Path A dataset, *Bull. Am. Meteorol. Soc.*, *78*(7), 1449–1472.

Swetnam, T. W., and J. L. Betancourt (1998), Mesoscale disturbance and ecological response to decadal climatic variability in the American southwest, *J. Clim.*, *11*, 3128–3147.

Thonicke, K., S. Venevsky, S. Sitch, and W. Cramer (2001), The role of fire disturbance for global vegetation dynamics: Coupling fire into a dynamic global vegetation model, *Global Ecol. Biogeogr.*, *10*(6), 661–677.

Townsend, A. R., P. M. Vitousek, and S. E. Trumbore (1995), Soil organic-matter dynamics along gradients in temperature and land-use on the islands of Hawaii, *Ecology*, *76*(3), 721–733.

Townsend, A. R., G. P. Asner, J. W. C. White, and P. P. Tans (2002), Land use effects on atmospheric ^{13}C imply a sizable terrestrial CO_2 sink in tropical latitudes, *Geophys. Res. Lett.*, *29*(10), 1426, doi:10.1029/2001GL013454.

Trolier, M., J. W. C. White, P. P. Tans, K. A. Masarie, and P. A. Gemery (1996), Monitoring the isotope composition of atmospheric CO_2: Measurements from the NOAA Global Air Sampling Network, *J. Geophys. Res.*, *101*(D20), 25,897–25,916.

Tucker, C. J., J. E. Pinzon, M. E. Brown, D. Slayback, E. W. Pak, R. Mahoney, E. Vermote, and E. L. Saleoous (2005), An extended AVHRR 8-km NDVI data set compatible with MODIS and SPOT vegetation NDVI data, *Int. J. Remote Sens.*, in press.

Van der Werf, G. R., J. T. Randerson, G. J. Collatz, and L. Giglio (2003), Carbon emissions from fires in tropical and subtropical ecosystems, *Global Change Biol.*, *9*(4), 547–562.

Van der Werf, G. R., J. T. Randerson, G. J. Collatz, L. Giglio, P. S. Kasibhatla, A. F. Arellano, S. C. Olsen, and E. S. Kasischke (2004), Continental-scale partitioning of fire emissions during the 1997 to 2001 El Niño/La Niña period, *Science*, *303*(5654), 73–76.

Veldkamp, E. (1994), Organic-carbon turnover in 3 tropical soils under pasture after deforestation, *Soil Sci. Soc. Am. J.*, *58*(1), 175–180.

Yevich, R., and J. A. Logan (2003), An assessment of biofuel use and burning of agricultural waste in the developing world, *Global Biogeochem. Cycles*, *17*(4), 1095, doi:10.1029/2002GB001952.

G. J. Collatz, NASA Goddard Space Flight Center, Code 923, Greenbelt, MD 20771, USA. (jim.collatz@nasa.gov)

R. S. DeFries and E. S. Kasischke, Department of Geography, University of Maryland, College Park, MD 20742, USA. (rdefries@mail.umd.edu; ekasisch@geog.umd.edu)

L. Giglio, Science Systems and Applications Inc., NASA Goddard Space Flight Center, Code 923, Greenbelt, MD 20771, USA. (giglio@hades.gsfc.nasa.gov)

P. Kasibhatla, Nicholas School of the Environment and Earth Sciences, Duke University, A355 LSRC, Box 90328, Durham, NC 27708, USA. (psk9@duke.edu)

J. B. Miller, NOAA Climate Monitoring Diagnostics Laboratory, 325 Broadway, Boulder, CO 80303, USA. (john.b.miller@noaa.gov)

J. T. Randerson, Department of Earth System Science, 3212 Croul Hall, University of California, Irvine, CA 92697-3100, USA. (jranders@uci.edu)

C. J. Still, Geography Department, 3611 Ellison Hall, University of California, Santa Barbara, CA 93106, USA. (still@icess.ucsb.edu)

G. R. van der Werf, Faculty of Earth and Life Sciences, Vrije Universiteit, De Boelelaan NL-1085, Amsterdam, Netherlands. (guido.van.der.werf@falw.vu.nl)

J. W. C. White, Cooperative Institute of Arctic and Alpine Research, University of Colorado, Boulder, CO 80309-0216, USA. (james.white@colorado.edu)